Elastic and inelastic scattering of ^{6}Li on ^{12}C

P. K. Bindal and K. Nagatani
Cyclotron Institute, Texas A & M University, College Station, Texas 77843*

M. J. Schneider† and P. D. Bond
Brookhaven National Laboratory,‡ Upton, New York 11973

(Received 28 February 1974)

Elastic and inelastic scattering of ^{6}Li on ^{12}C were studied at 36.4 MeV and 40.0 MeV incident energies. Previously published elastic scattering data for 20, 24.5, 28, 30.6, and 63 MeV incident energies as well as the present data were analyzed to obtain an energy dependent optical potential. Inelastic scattering was measured for the transitions to the states at 4.44 MeV (2^{+}), 7.65 MeV (0^{+}), 9.63 MeV (3^{-}), 10.84 MeV (1^{-}), 11.83 MeV (2^{-}), 12.71 MeV (1^{+}), 13.35 MeV (2^{-}), and 14.05 MeV (4^{+}) in ^{12}C. The angular distributions were analyzed using the distorted wave Born approximation with the usual collective form factor. Various options for the form factors and the optical potentials were investigated. It is found that the use of complex form factors generally fits the data. Results of these calculations are presented for all transitions and the values of β are deduced. For the transition to the 4.44 MeV (2^{+}) state, both the shape and magnitude of the angular distribution (and hence the state's deformation parameter β_2) were well reproduced.

[NUCLEAR REACTIONS ^{12}C(^{6}Li, ^{6}Li), (^{6}Li, ^{6}Li'), E = 36.4 and 40.0 MeV; measured $\sigma(\theta)$, deduced energy-dependent optical-model parameters for E = 20–63 MeV; DWBA analysis, deduced deformation parameters β_L.]

I. INTRODUCTION

The investigation of heavy ion elastic scattering has a long history and there exist a vast number of extensive surveys. Heavy ion transfer reactions have also been a popular subject, not only because of the inherent interest in understanding the reaction mechanism but also for their potential use in extracting structure information. Besides the study of Coulomb excitation, on the other hand, relatively limited activity has been reported in heavy ion inelastic scattering. Garvey *et al.*,[1] in 1962, showed interesting and important features involved in inelastic scattering. Recent studies[2] of Coulomb-nuclear interference effects[3] have also demonstrated an interesting use of the inelastic scattering of heavy ions around the Coulomb barrier.

Besides these potentially interesting implications, there are also practical reasons for pursuing the study of inelastic scattering. The application of the ordinary distorted wave Born approximation (DWBA) to heavy ion inelastic scattering should be explored in order to realize its validity. It should be remembered that the use of the usual macroscopic collective form factor eliminates many difficulties encountered in heavy ion processes, for instance, finite range treatment, recoil effects, etc. The information about strong inelastic channels provides input data to coupled channel calculations for transfer reactions.

With these considerations, the elastic and inelastic scattering of ^{6}Li on ^{12}C was measured at 36.4 and 40.0 MeV incident energies. The target ^{12}C was chosen for the following reasons: there are numerous experimental[4-6] and theoretical[7] investigations using light projectiles on ^{12}C, the structure of ^{12}C is very well known (in particular, there are collective type states which are well suited for the present analysis), there are unnatural parity states which could be good testing examples for the spin dependent treatment, and the 0^{+} at 7.65 MeV and the 4^{+} at 14.05 MeV states can be used in a search for higher order processes.[8]

In the present DWBA analysis, the emphasis was on carrying out a thorough check of dependences on several parameters, not just obtaining best fits to the data. In order to pursue such an analysis, the optical potential for the elastic scattering had to be obtained, although there are many such studies reported in the literature.[9-13] It was especially important to have a proper energy dependence in the optical potential, since for the highly excited states the energy difference between the incident and outgoing channels becomes large in the inelastic processes. Consequently, the distorted waves generated may be considerably different. In order to extract such effects and to obtain the proper potential all available

elastic data were utilized in addition to the present results.

With a ^{6}Li projectile, there is more than one possible mode for an inelastic transition because several transferred angular momenta can couple with the 1^+ ground state of ^{6}Li to make a given spin-parity change. Such couplings can be calculated unambiguously only when the spin-orbit interaction is known. In the present analysis, it was not possible to perform such an unambiguous calculation due to a lack of reliable information about the spin-orbit interaction, however, the effect of the mixing of transferred angular momenta is discussed.

The 2^+ state at 4.44 MeV and 3^- state at 9.63 MeV were extensively used to make a thorough test of the DWBA since they are the best candidates for the collective form factor treatment. The other states observed were the 7.65 MeV (0^+), 10.84 MeV (1^-), 11.83 MeV (2^-), 12.71 MeV (1^+), 13.35 MeV (2^-), and 14.04 MeV (4^+) states, and they were analyzed in a somewhat more restricted manner. In the next section, the experimental procedures are briefly described. In Sec. III, the elastic scattering analysis is presented followed by a description of the inelastic scattering in Sec. IV.

II. EXPERIMENTAL PROCEDURE

Using the Brookhaven tandem facility, two sets of experiments were carried out at incident energies of 36.4 and 40.0 MeV. A beam of $^6Li^{3+}$ was obtained from one of the MP tandems with a typical intensity of 200 nA. A natural carbon target whose thickness was measured by an α source to be 200 ± 30 μg/cm^2 was used. Two solid state counter telescopes, with 25 μm and 300 μm detectors as ΔE and E counters, respectively, were used. The over-all energy resolution was typically 200 keV as is seen in Fig. 1. Beam was collected in a Faraday cup and its intensity was monitored in addition by a monitor detector. The identification of ^{6}Li was made using an electronic multiplier, and spectra were stored in the on-line Sigma-7 computer. The cross sections were obtained by conventional analysis and the angular distributions obtained are shown in the next sections. The uncertainties estimated in the absolute cross sections are within 20%.

III. OPTICAL MODEL ANALYSIS FOR ELASTIC SCATTERING

All available data on the elastic scattering of ^{6}Li on ^{12}C were collected and analyzed on an equal footing. The procedure, though it is standard, is briefly reviewed. The Woods-Saxon optical potential is given by

$$U(r) = -V_0 \frac{1}{1+\exp(r-R_r/a_r)} - iW_0 \frac{1}{1+\exp(r-R_i/a_i)} + V_C(r), \quad (1)$$

where the Coulomb potential $V_C(r)$ is calculated as usual, using

$$V_C(r) = \frac{Z_1 Z_2 e^2}{2R_c}\left(3 - \frac{r^2}{R_c^2}\right), \quad r \leq R_c$$

$$= \frac{Z_1 Z_2 e^2}{r}, \quad r > R_c .$$

The notation used here is standard, and the radius parameters R_r, R_i, and R_c are defined by R

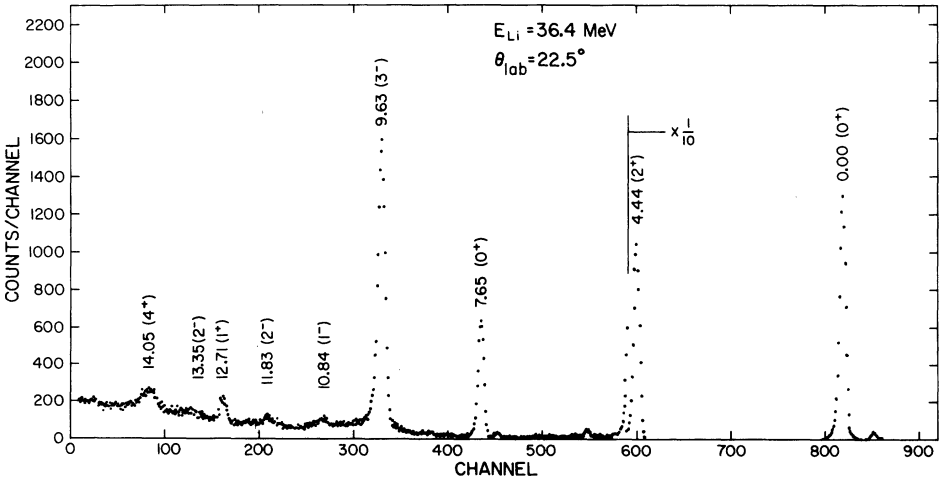

FIG. 1. The ^{6}Li spectrum of ^{12}C(^{6}Li, ^{6}Li')^{12}C* at $\theta_{lab} = 22.5°$. The excitation energy with spin and parity of each state in ^{12}C studied in the present analysis is given.

$=r_0(A_1^{1/3}+A_2^{1/3})$. (Another convention, $R=r_0A_2^{1/3}$ has become quite commonly used, especially for ^{6}Li, but a more traditional definition is adopted here.) The angular distributions were calculated using a computer program JIB 6[14] for the parameter search, with the usual merit criterion, minimization of the quantity

$$\chi^2=\frac{1}{n}\sum_{i=1}^{n}\{[\sigma_{th}(\theta_i)-\sigma_{exp}(\theta_i)]/\Delta\sigma_{exp}(\theta_i)\}^2.$$

In the actual search, one more simplification was made by fixing the Coulomb radius parameter r_C = 1.35 fm, because the variation in cross section due to changes in this parameter is known to be small.[11] Thus the variation of six parameters was studied.

Prior to the present study, there were several investigations of the elastic scattering, i.e., at incident energies of 20,[9] 24.5,[10] 28,[11] 30.6,[12] and 63 MeV.[13] The optical model analyses had been carried out for all of these data except for the 63 MeV case. It is noted, however, that there are large differences in the depths of the real and imaginary parts among these analyses. Bassani *et al.*[11] made an extensive analysis for the 24.5, 28, and 30.6 MeV data, but while excellent fits were obtained to the data at each energy, the parameters change in an irregular fashion for different energies. Therefore, they are not suitable for the present purpose as the need for a consistent potential over a wide energy range was discussed in the Introduction. Accordingly, a search

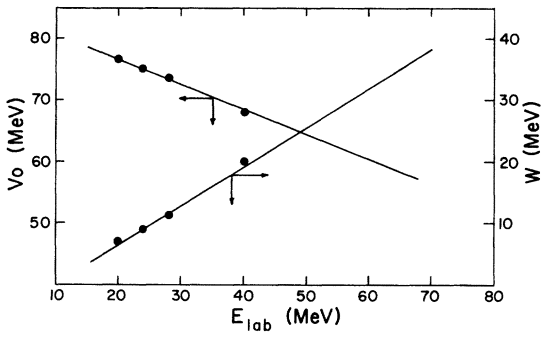

FIG. 2.

$$V(r)=V_0\frac{-1}{1+\exp(r-R_r/a_r)}+iW_0\frac{-1}{1+\exp(r-R_i/a_i)}+V_c,$$

$V_0=85.2-0.64E_{\text{c.m.}}$ (MeV),

$W_0=-6.4+0.96E_{\text{c.m.}}$ (MeV),

$r_r=0.97$ (fm), $a_r=0.735$ (fm),

$r_i=1.25$ (fm), $a_i=0.386$ (fm),

$r_c=1.35$ (fm).

Optical potential parameters and linear energy dependence of the depths of the real and imaginary parts.

was made to fit all the data mentioned above in addition to the present results with one set of parameters.

The actual procedure to find the optical potential was performed in several steps. First, a χ^2 fit was carried out by varying all six parameters for the 28 MeV data. Then the 20, 24.5, and 40.0 MeV data were fitted by varying only the depths of the real and imaginary parts simultaneously. The results are summarized in Fig. 2. In the upper half of this figure, the depths of the real and imaginary parts are denoted by solid points. It is noted from these points that the variations in these depths are very closely approximated by linear energy dependences, as represented by the lines drawn through the points. The parameters thus obtained are displayed in the lower half of the figure. The feature that the real depth decreases while the imaginary depth increases with increasing energy can be understood as the opening of more channels at higher energies. The linear dependences[15] are the simplest approximation for such effects.

The potential obtained was then subjected to comparison with the rest of the data, i.e., the angular distributions for incident energies of 30.6, 36.4, and 63 MeV were calculated. The first two cases were reproduced quite well. However, while the shape of the angular distribution of the 63 MeV data was reproduced well, the calculated magnitude was too large by a factor of 3.5 compared to the experimental data. The original result was quoted with an accuracy of 10–20% in its absolute cross section.[13] It is not easily understood that the potential explaining the data from 20 to 40 MeV with a reasonable accuracy in reproducing the magnitude of the cross section can miss the data at 63 MeV by such a large factor. It was also found, as described later, that when the inelastic transition to the 2^+ state at 4.44 MeV obtained in the same measurement was calculated with the present optical potential, it too disagreed by the same factor. Under these circumstances, it was decided that no conclusion could be made as to the absolute cross sections for this set of data, and the discrepancy was ignored. In the results presented here, therefore, the experimental data were renormalized to the calculated cross sections.

The calculated angular distributions for all seven cases are displayed with the data in Fig. 3. Individual fits could have been improved slightly by adjusting the parameters but it is important to note the over-all agreement for such a wide energy range with a single energy dependent parameter set. The χ^2's were typically 10–50 including all data points although the absolute estimates of χ^2 are not easily made as the experi-

mental errors are hard to extract from the published figures. Several features of the comparison of calculated results to experimental data should be mentioned. In general, the backward angles were poorly reproduced. For instance, in the case of 30.6 MeV data, the deviation grows very large beyond $\theta_{c.m.} \approx 110°$. This may suggest that a more complicated treatment is necessary. On the other hand, it is interesting to note that a use of very deep potentials with depths V_0 ranging from 200–460 MeV did reproduce this backward rise.[11] For the 20 MeV data, where the fit also becomes poor at backward angles, a shallower potential with a depth of $V_0 = 53.6$ MeV (with all other parameters in the present optical potential unchanged) gave a better fit to the experimental data, as good a fit as obtained by Bethge, Meier-Ewert, and Pfeiffer.[9]

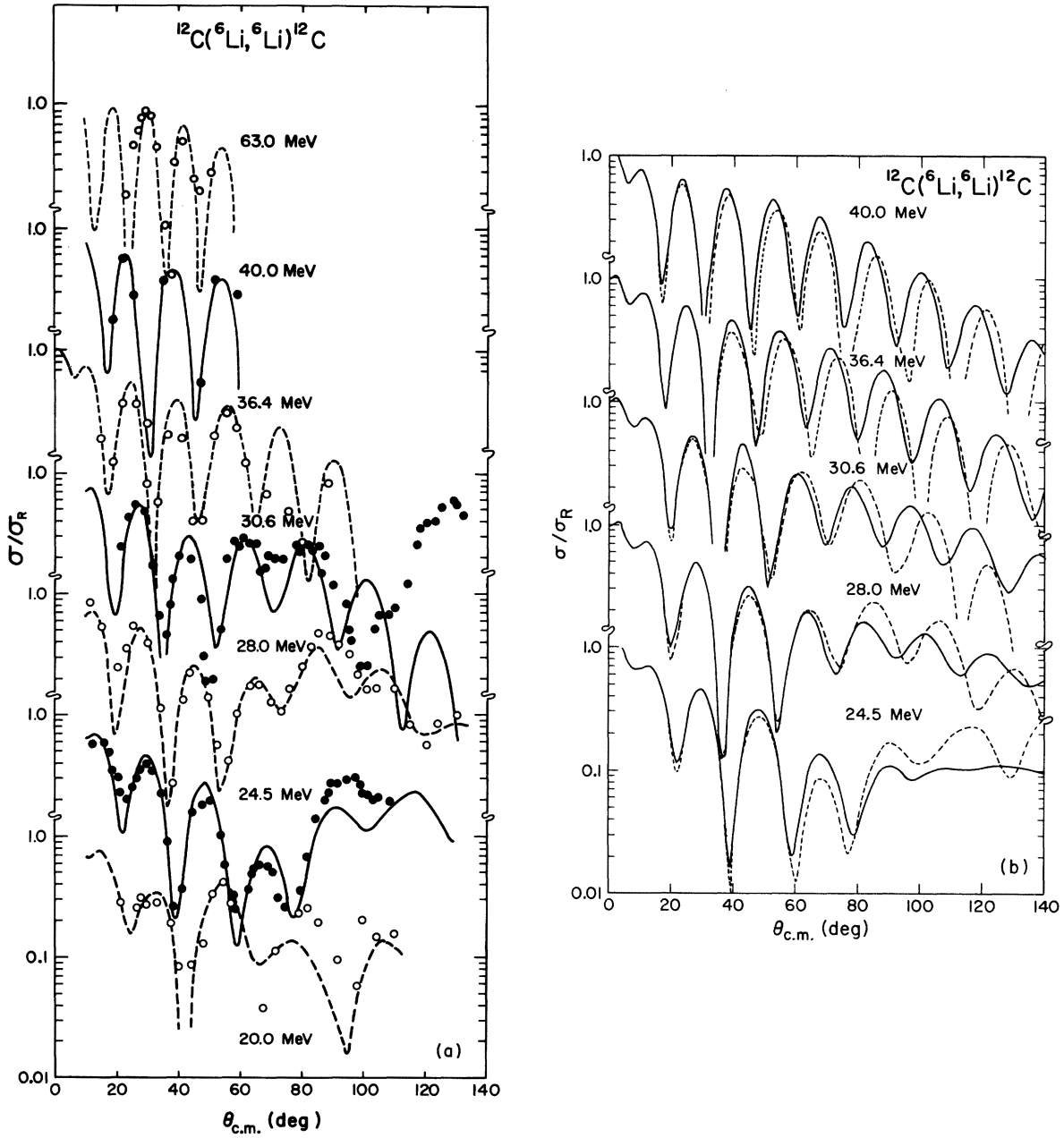

FIG. 3. (a) Comparison of the experimental elastic differential cross sections with those calculated by using the parameters of Fig. 2. (b) Comparison of calculated elastic scattering cross sections with no spin-orbit strength (dashed curve) and with $V_{so} = 7.5$ MeV (solid curve).

To investigate the influence of the spin-orbit interaction, we calculated the elastic scattering differential cross sections for energies of 24.5, 28, 30.6, 36.4, and 40.0 MeV. The standard Thomas form for the spin-orbit potential was used with $V_{so} = 7.5$ MeV (the imaginary term was chosen to be zero). Results are shown in Fig. 3(b). At angles up to about 60° (c.m.) the effect of the spin-orbit term is small whereas at large angles the change in the cross section is more pronounced. It should be noted that the inclusion of the spin-orbit term does not improve the fit to the lower energy elastic data at large angles. For this reason and because much of the data does not extend to large enough angles, the spin-orbit term is not included in the rest of the analysis.

As a whole, the potential generated in the present study is very satisfactory to explain the elastic data ranging from at least 24 MeV to at least 40 MeV. The detailed agreements are still not precise, especially for the backward angles, but again more experimental data are required to make quantitative investigations. The discrepancy between the experimental and the calculated absolute cross sections at 63 MeV is very disturbing, and additional experimental measurement at higher energy is strongly suggested.

IV. INELASTIC SCATTERING AND DWBA ANALYSIS

Angular distributions were measured for eight transitions to excited states in ^{12}C. A typical energy spectrum showing these levels is presented in Fig. 1, and the angular distributions are shown in the succeeding figures. Additional information was also available from the measurements by Ollerhead, Chasman, and Bromley[13] for the 4.44 MeV state at 63 MeV bombardment.

In the DWBA analysis, 100 partial waves were used and were found to be adequate. Coulomb interference is not a critical problem over the angle range dealt with.[16] As already mentioned, the macroscopic collective model is used to calculate the form factor, and a brief description is given here to clarify the discussion. The optical potential is assumed to be deformed, and the nuclear radius is described by a multipole expansion $R = R_0[1 + \sum_{LM} \beta_L Y_{LM}(\theta, \phi)]$. The deformation parameter β_L, which plays a vital role, is introduced. A magnitude of β_L extracted in the present analysis can be compared to the value obtained previously from the analysis better studied reactions, e.g., (p, p'). Then the degree of agreement would provide a measure of goodness of the present analysis. Using this deformed radius, the optical potential is expanded in a Taylor series as

$$U(r - R) = U(r - R_0) - R_0 \frac{\partial}{\partial r} U(r - R_0) \sum_{LM} \beta_L Y_{LM}(\theta, \phi) + \cdots . \quad (2)$$

The interaction potential responsible for the transition is the second term, i.e., the derivative of the optical potential. Higher order terms could also be important and will be discussed.

Having the formalism established, several options in the actual calculation can be explicitly listed:

1. (a) The form factor is calculated from the real part of the optical potential.
   (b) The form factor is calculated from the whole complex optical potential.
2. (a) The distorted waves in the outgoing channel are evaluated with the potential used for the incident energy (this is the usual practice).
   (b) The distorted waves in the outgoing channel are evaluated with the appropriate potential for the proper exit channel energy. As repeatedly mentioned, this treatment must be the proper method, since the optical potential is energy dependent.
3. (a) The form factor is calculated from the potential at the incident energy.
   (b) The form factor is calculated from the potential at the outgoing energy.
   (c) The form factor is calculated from the potential at some intermediate energy.
4. (a) A transition is calculated without the mixing of possible angular momentum transfers due to nonzero spin transfers.
   (b) A transition is calculated with such mixing.

It is obvious that a complete investigation to cover all these alternatives for all the states is not feasible. Therefore, a systematic survey is performed for the 2^+ and 3^- states at 4.44 and 9.63 MeV, respectively. The rest of the states are analyzed in a more restricted frame.

2^+ state at 4.44 MeV

The calculated results together with the experimental data for 36.4, 40.0, and 63 MeV incident energies are shown in Fig. 4. The measured cross sections are plotted with error bars which are only statistical uncertainties. The estimated uncertainties in the absolute cross section are within 20% for the present results. In the 63 MeV data, the absolute cross section was renormalized by the factor of 3.5 as discussed in the previous section.

It should be remembered that the spin-orbit interaction was not used in the optical potential.

This then eliminates any quantitative analysis which includes the mixing of different angular momentum transfers. For the transition to the 2^+ state, the orbital angular momentum transfer, ΔL, is equal to 2 only in the absence of spin transfer, ΔS.

In each figure, there are four theoretical curves displayed, as follows:
(i) solid curves using the complex form factor [1(b)], and the different outgoing distorted waves, i.e., evaluated from the potential at the proper channel energy [2(b)];
(ii) dotted curves using the real form factor [1(a)], and the different outgoing distorted waves [2(b)];
(iii) dash-dotted curves using the complex form factor [1(b)], and the same outgoing distorted waves, i.e., evaluated from the potential at the incident energy [2(a)];
(iv) dash curves using the real form factor [1(a)], and the same outgoing distorted waves [2(a)].
All these were calculated with the form factors at the incident energies [option 3(a)], and the discussion of the variation due to this option is given below.

The calculated angular distributions are normalized to the experimental data at $\theta_{c.m.} \approx 30^\circ$. A few observations can be made about the shapes of the angular distributions using different options. In the case of 36.4 MeV, the calculated shapes using the real form factor do not show any differences up to $\theta_{c.m.} \approx 60^\circ$ for the different choices of the outgoing distorted waves (curves ii and iv in the figure). At further backward angles, they start showing some deviation from each other in slope. The only difference in the calculations with the complex form factor, however (curves i and iii in the figure), is the depth of the minima. For the cases of higher incident energies, general features of the shapes of the angular distributions are also reproduced. In the case of the calculations for the 40.0 MeV incident energy, a distinction can be made in the curves for the real form factor and complex form factor, however, distinction between the different choices of the outgoing distorted waves with same form factor is hard to make for almost the whole angular distribution. The same is true for the case of 63 MeV calculations. Additional difficulties are encountered for this case. The minima produced by the calculations seem to be sharper than the experimental data. Unfortunately, it is difficult to make any conclusion as to a selection of these alternative calculations by comparing with the data as seen in the figures. Furthermore, the agreement with the experimental data is not excellent in the case of 36.4 MeV, although reproduction of maxima and minima is reasonably good.

It should naturally be expected that the mixing of different angular momentum transfers could change the shapes. In order to demonstrate this effect, the angular distributions, using the complex form factor [option 1(b)] and the different outgoing distorted waves [option 2(b)], were calculated for the transitions with $\Delta L = 0$ and $\Delta S = 2$,

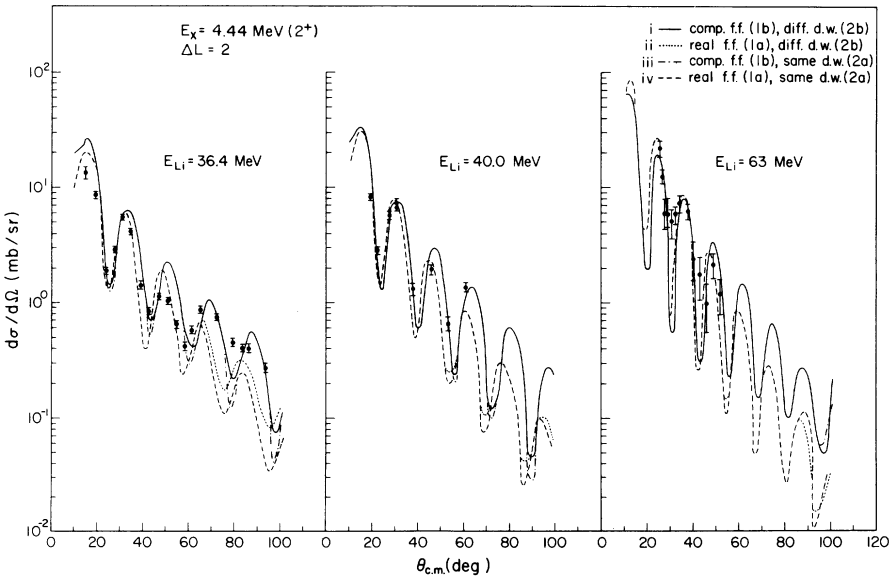

FIG. 4. Experimental cross sections and the DWBA fits for the 2^+ state in ^{12}C. Shown in this figure are also the comparisons of the different options of the form factors and the optical potentials to calculate distorted waves in the outgoing channel.

and $\Delta L = 4$ and $\Delta S = 2$. The relative shapes of the three cases, $\Delta L = 2$, $\Delta L = 0$, and $\Delta L = 4$, are displayed in Fig. 5. A sum of these curves with certain relative strengths might improve the fit to the experimental data; however as discussed above, it would have little meaning. Moreover, since coherent interference due to these different modes could change the detailed shape much more even if the mixing were small, no further investigation concerning the mixing effects was made.

The absolute cross sections yielded more interesting results, which are discussed next. The values of β_2 were extracted, as usual, by comparing the calculated cross sections to the experimental cross sections. The β values obtained were then corrected by multiplying a factor $(12^{1/3} + 6^{1/3})/12^{1/3}$ so that they could be directly compared to the ones obtained from light projectile inelastic scattering, say (p, p'). The results are summarized in Table I. There are four values listed for each incident energy case according to the four different calculations as in Fig. 4. Several interesting features can be pointed out from an observation of the results. The β_2 values are roughly constant for different incident energy cases, provided again that renormalization of the 63 MeV data is allowed, for the complex form factor calculations. On the other hand, they vary greatly when the real form factor is used in the calculation. This type of large discrepancy in the β value has been noted,[17] where use of the real form factor gave unacceptably large values of β. The difference due to the choice of the outgoing distorted waves is found to be only 4–8%. The use of the same distorted waves yields consistently higher β_2 values.

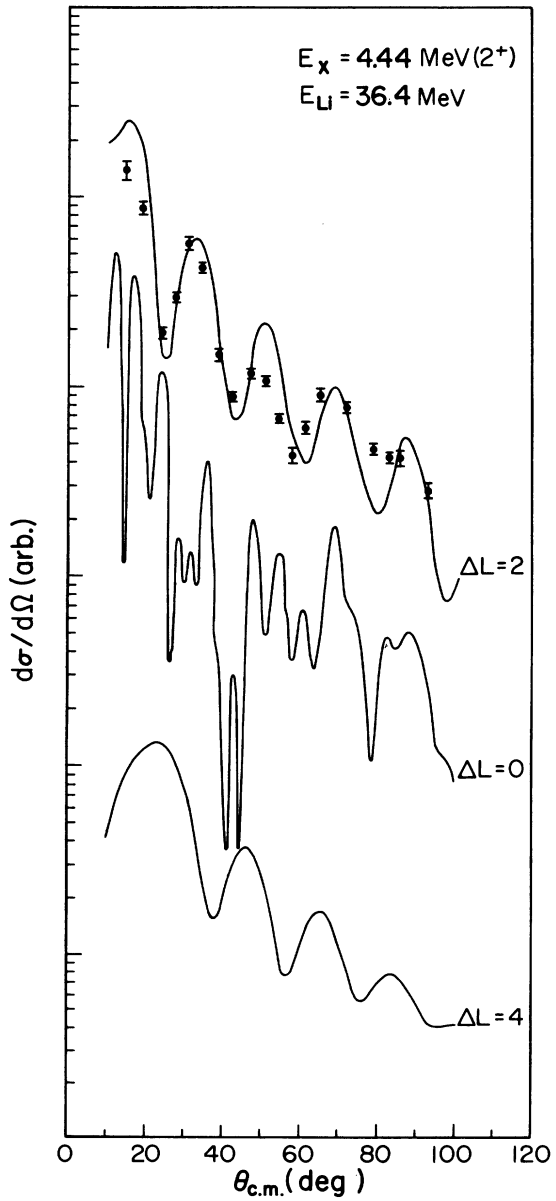

FIG. 5. Relative shapes for the 2^+ state are displayed by using $\Delta L = 2$, $\Delta S = 0$; $\Delta L = 0$, $\Delta S = 2$; and $\Delta L = 4$, $\Delta S = 2$ transfers.

In comparing the present result to the other studies, the value of $\beta_2 R$ should be used.[18] Values ranging from 1.4 to 1.7 fm have been reported by Satchler[7] in the analysis of (p, p') and a value of 1.2 ± 0.4 fm was given by von Oertzen *et al.* from the analysis of the $(^{14}N, ^{14}N')$ reaction.[19] Several other values clustering around 1.5 and 1.6 have also been determined by different means.[5,20,21] From the present results, the value of 1.1 to 1.5 fm can be extracted using the complex form factor depending on whether the real or imaginary radius is used.

3^- state at 9.63 MeV

Figures 6(a) and 6(b) show the experimental cross section data together with the calculated results for the 36.4 and 40 MeV incident energies, respectively. In each figure, there are four calculated curves and the legend used for these curves is the same as is used for the 2^+ state at

TABLE I. Values of the deformation parameter β_2 obtained for the 2^+ state at 4.44 MeV.

Form factor [a] option	DW [a] option	E_{Li} (MeV) 36.4	40.0	63
Real [1(a)]	Same [2(a)]	0.57	0.62	1.15
Comp [1(b)]	Same [2(a)]	0.54	0.52	0.53
Real [1(a)]	Diff [2(b)]	0.53	0.61	1.05
Comp [1(b)]	Diff [2(b)]	0.50	0.49	0.51

[a] Labeled as explained in text.

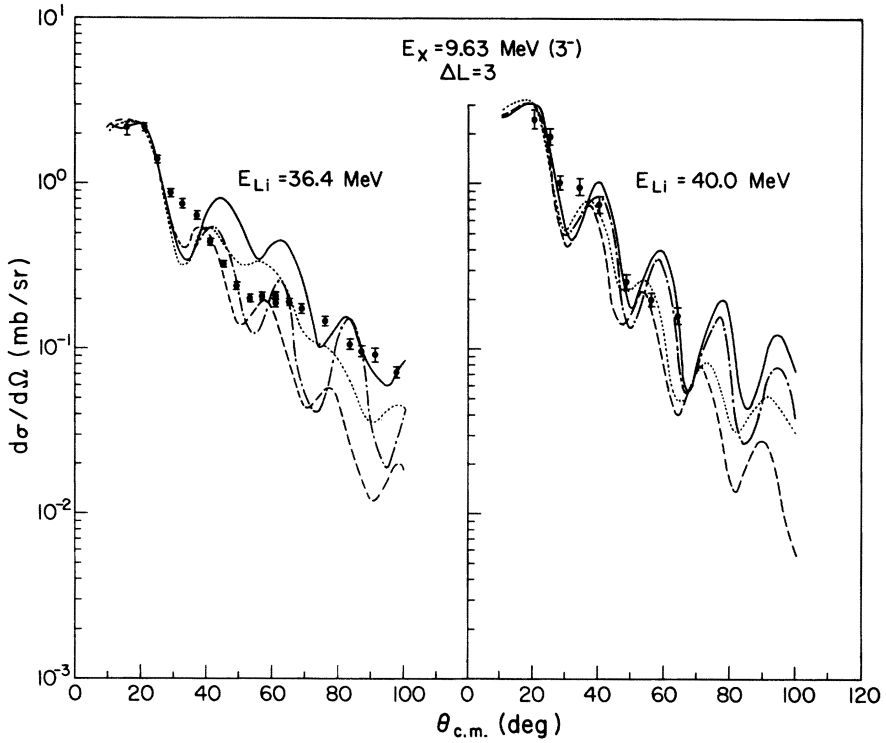

FIG. 6. Experimental cross sections and the DWBA fits for the 3^- state in ^{12}C. Legend used for the theoretical curves is the same as used in Fig. 4.

4.44 MeV. The calculated curves are normalized to the experimental data at $\theta_{c.m.} \approx 20°$. In both cases, experimental data show much less structure than the calculated curves.

In the case of 40.0 MeV, the calculated curves using complex form factors show quite similar shapes for the different choices of the optical potentials in the outgoing channels [curves i and iii in Fig. 6(b)]. That is also the case for the choice of real form factor (curves ii and iv). In the case of 36.4 MeV, the differences are more enhanced. None of the calculated curves, however, seems to fit the data very well. Calculations for both the 36.4 MeV and the 40.0 MeV cases show that there should be a minimum at about $\theta_{c.m.} \approx 32°$ which is missing in the experimental data. The reason for this discrepancy may still be due to insufficient description of the outgoing optical potential (at $E_{Li} = 22$ MeV) for the 36.4 MeV data since the present set of parameters starts showing deviation at $E_{Li} = 20$ MeV data (see Fig. 2). For this reason, in the exit channel, we tried a number of sets of optical potentials that fit experimental data at 20 MeV. Although the fit to the data was slightly improved, sharp minima at about $\theta_{c.m.} \approx 32°$ always appeared in the calculations.

This 3^- state and other states could have contributions from the second-order term in the expansion (2) as well as any other effects. Calculations[8] show that when a coherent sum of both the first-order and second-order interaction terms is used, the shapes of the angular distributions for the 2^+ state at 4.44 MeV and the 3^- state at 9.63 MeV do not change appreciably. On the other hand, the mixing of angular momentum transfers due to the nonzero spin transfer would certainly change the shape but unfortunately this calculation is beyond the scope of the present work.

The β_3 values obtained from the fits shown in Fig. 6 are given in Table II. The same conclusions can be drawn about the trend in values of this deformation parameter as for the β_2 parameter dis-

TABLE II. Values of the deformation parameter β_3 obtained for the 3^- state at 9.63 MeV.

Form factor [a] option	DW [a] option	E_{Li} (MeV) 36.4	40.0
Real [1(a)]	Same [2(a)]	0.34	0.38
Comp [1(b)]	Same [2(a)]	0.33	0.32
Real [1(a)]	Diff [2(b)]	0.28	0.32
Comp [1(b)]	Diff [2(b)]	0.27	0.27

[a] Labeled as explained in text.

cussed above. One interesting observation from Tables I and II is that the values of β_2 and β_3 extracted from the study of 36.4 MeV data are about equal regardless of the choice of the form factor. The differences in the values start increasing with the increase of incident energy for the real form factor. This probably indicates that the imaginary form factor starts dominating at higher incident energies. It will be interesting to study inelastic scattering at lower energies and compare these values of β_L. At present no published data exist in that region.

The value of $\beta_3 R$, using the complex form factor and the same optical potentials in the entrance and the exit channels [option 2(a)], lies between 0.73 and 0.94 fm, depending on the choice of the real or imaginary radius. These values are slightly lower than those obtained by Satchler[7] for (p, p') which range from 0.98 to 1.15 fm. Hinterberger *et al.*[5] obtain $\beta_3 R = 0.97$ fm from the (d, d') study. If the energy dependent potential in the exit channel is used, the value of $\beta_3 R$ is reduced by 18% in the present analysis.

In order to study the effect of options (3) calculations were carried out by using 3(c) where the complex form factor is calculated from the potential at an energy midway between the entrance and exit channel energies. The shapes of the angular distributions for both the 2^+ state at 4.44 MeV and the 3^- state at 9.63 MeV did not change appreciably as compared to those displayed as solid curves in Figs. 4 and 6. However, in both cases, the cross section was reduced which in turn gave a 4% increase in the values of β_2 and β_3.

Other negative parity states

In Fig. 7 angular distributions for the 1^- state at 10.84 MeV, the 2^- state at 11.83 MeV, and the probable 2^- state at 13.35 MeV using 40.0 MeV incident beam are displayed. These are weak states and the statistical errors are large. In the case of 13.35 MeV excitation, the data represent an estimate of the upper limit as the statistical errors are very large.

For the 1^- state at 10.84 MeV the dipole term simply represents a shift of the center of mass of the nucleus since it is a $T=0$ state. Although the excitation of the 1^-, $T=0$ state cannot be explained in the framework of the present treatment, the collective model form factor was applied in the absence of a better model.

This state could also be excited legitimately with the $\Delta L = 3$ and $\Delta S = 2$ transfer. The angular distribution calculated using $\Delta L = 3$ is shown in Fig. 7(a). The extracted value of β_3 is 0.16 if the same normalization is used as for the $\Delta S = 0$

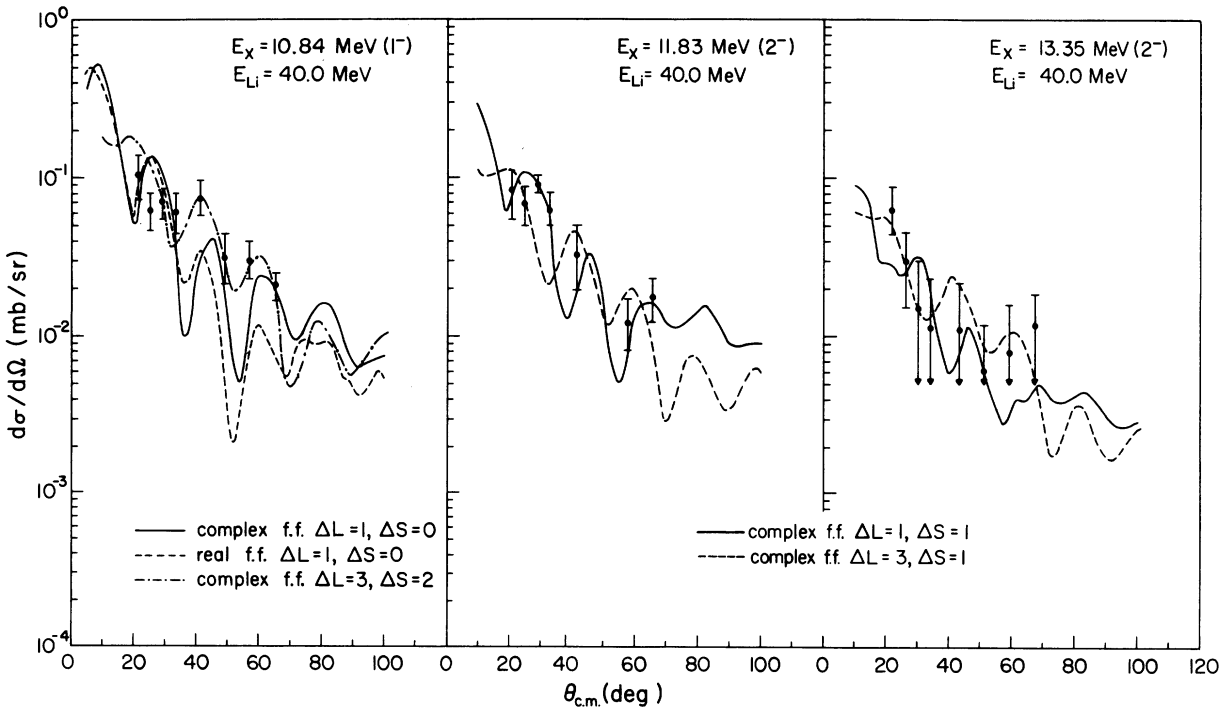

FIG. 7. Experimental cross sections and DWBA results for states in ^{12}C. The comparisons with different choices of the form factors and the different options of the angular momentum transfers are also shown.

transfer cases. This transfer is allowed only for spin-one particles. However, this state is also excited by using protons[4] and ^{3}He[5] where $\Delta L = 3$ is not allowed.

The 2^- unnatural parity states at 11.83 and 13.35 MeV can be excited with $\Delta L = 1$, $\Delta S = 1$ or 2, and $\Delta L = 3$, $\Delta S = 1$ or 2 transfers. The calculated angular distributions for $\Delta L = 1$ and $\Delta L = 3$ are shown in Figs. 7(b) and 7(c) for these two states. For the 11.83 MeV state, values of $\beta_1 = 0.11$ and $\beta_3 = 0.13$ are obtained if the same normalization as for $\Delta S = 0$ is used. In the case of the 13.35 MeV state the upper limits on the values of β_1 and β_3 are 0.07 and 0.10, respectively.

7.65 and 14.05 MeV states

In Figs. 8 and 9 the angular distributions for the 0^+ state at 7.65 MeV and the 4^+ state at 14.05 MeV are displayed for the incident energies of 36.4 and 40.0 MeV. The data for 0^+ states show an angular distribution similar to the 2^+ state whereas the data for the 4^+ state for 36.4 MeV incident energy show a flat structureless distribution.

The $\Delta L = 0$ transfer calculation as shown in Fig. 8 does not reproduce the data, as the calculated curve shows a more oscillatory pattern. Similarly, the $\Delta L = 4$ transfer calculations as shown in Fig. 9 do not fit the data for the 14.05 MeV state. The calculated curves using the same optical potential in the exit channel as in the entrance channel show a large slope. The curves shown here are calculated by using a complex form factor and the value of $\beta_4 = 0.20$ is used to obtain the cross section. Use of a real form factor gives curves with much larger slopes. Since the energy dependent potentials obtained in the present study may not be successful in reproducing the elastic scattering data between 15–20 MeV incident energies, calculations using this potential in the exit channel are not presented. However, use of other available potentials for $E_{Li} = 20$ MeV in the exit channel did not improve the fits.

The second-order term in the expansion (2) may be important for this state. Calculations[8] show that the shape of the calculated curve using this term alone gives an angular distribution that has a large slope and also that the curve calculated by using a coherent sum of both the first-order and the second-order terms does not improve the fits also. There is an alternative method of describing the excitation of the 0^+ state and the 4^+ state; i.e., these states are populated by multiple excitation, for example, via the strongly excited 2^+ state at 4.44 MeV. The calculations do reproduce the shapes of the angular distributions and will be reported elsewhere.[8]

12.71 MeV state

This is a 1^+, $T = 0$ unnatural parity state, which can be excited only with a $\Delta S = 1$ or 2 spin transfer. This would imply that the angular momentum $\Delta L = 0$ or 2 is allowed in the present case. Using a purely central interaction in a microscopic description for this state, one expects monopole $\Delta L = 0$ contribution to dominate over the quadrupole $\Delta L = 2$ contribution by a factor of 8. However, it has been found from the analysis of the inelastic scattering of 45.5 MeV protons that the $\Delta L = 2$ transfer with $\Delta S = 1$ gives reasonable fit to the data in the forward direction.[7] Microscopic calcu-

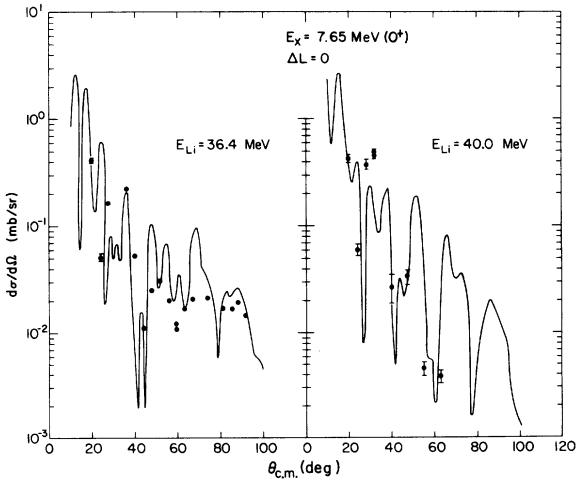

FIG. 8. Experimental cross sections for the 0^+ state in ^{12}C. The DWBA results were calculated by using option 2(b) discussed in the text.

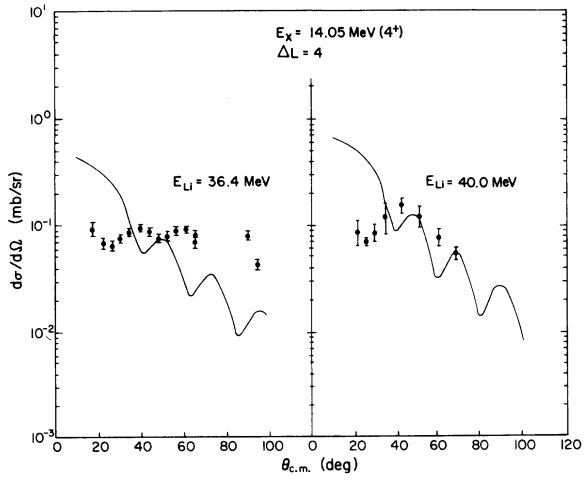

FIG. 9. Experimental cross sections for the 4^+ state in ^{12}C. The DWBA results were calculated by using option 2(a) as discussed in the text.

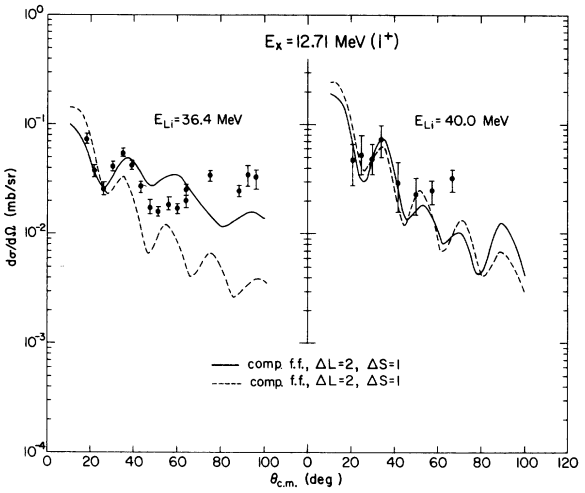

FIG. 10. Experimental cross sections for the 12.71 MeV state in ^{12}C. The DWBA results were calculated by using option 2(a) (dashed curve) and option 2(b) (solid curve).

lations of Love and Parish[22] showed that a tensor interaction term introduces a significant $\Delta L = 2$ amplitude in the forward direction and dominated over the $\Delta L = 0$ amplitude at larger angles. The situation is not clear for a composite spin-one projectile like ^6Li. The calculated results for $\Delta L = 2$ are displayed in Fig. 10. The $\Delta L = 0$ transfer gives too much oscillation in the angular distribution as in Fig. 8. The fit to the data with $\Delta L = 2$ transfer is reasonable. The results with $\Delta S = 1$ or $\Delta S = 2$ transfer show the same shape as the spin-orbit coupling term is absent in the optical potentials. This case may be a good example of where a spin-orbit term could be tried to fit the data. If the same normalization as for the $\Delta S = 0$ transfer is used, the effective deformation parameter is $\beta_2 = 0.14$ for a $\Delta L = 2$ and $\Delta S = 1$ transfer, which is in excellent agreement with Satchler's result[7] of $\beta_2 = 0.15$ using the (p, p') reaction.

IV. CONCLUSIONS

The elastic scattering data of ^6Li on ^{12}C for the incident energies of 20, 24.5, 28, 30.6, 36.4, 40.0, and 63 MeV are fitted using an energy dependent potential. Difficulties were encountered in fitting the two limiting cases, namely the 20 and 63 MeV data. The 20 MeV data up to $\theta_{c.m.} \approx 60°$ are reproduced rather well; however at larger angles, success is marginal. In the case of 63 MeV data, the shape of the angular distribution is reproduced but the magnitude of the experimental data must be multiplied by a factor of 3.5 to agree with the calculated data. The fits to the other data are found to be good so it appears that this optical potential is probably quite good in reproducing elastic scattering data for the incident energies between 20 and 63 MeV.

The ordinary distorted wave Born approximation using a simple collective model interaction [Eq. (2)] was utilized to calculate the inelastic scattering. It is found that the use of a complex form factor produced a consistently better fit to the inelastic scattering data for the 2^+ state at 4.44 MeV at incident energies of 36.4, 40.0, and 63 MeV than use of a real form factor. The superiority was not only in fitting the shape of the angular distribution but also in reproducing its magnitude. If an increase in the magnitude of the experimental data for the 63 MeV case by a factor of 3.5 as required from fitting the elastic scattering is allowed, consistent values of β_2, the deformation parameter, are obtained at all three energies. On the other hand, use of the real form factor gives unacceptably large values of β_2. It seems that the imaginary part of the form factor dominates at higher incident energies. Unfortunately, a distinction between the fits due to choice of the outgoing distorted waves could not be made, although use of the same optical potential in the exit channel as in the incoming channel yields consistently higher β_2 values.

In the case of octopole excitation, success in fitting the data for the incident energies of 36.4 and 40.0 MeV was limited. The calculated angular distribution shows a sharp minimum around $\theta_{c.m.} \approx 32°$ which is missing in the experimental data. Use of complex form factor does reproduce the value of β_3 consistently.

Nonzero spin transfers are needed to interpret unnatural parity states. Reasonable success has been achieved in fitting these states. For the 1^- state at 10.84 MeV, which should not be excited with dipole excitation, use of $\Delta L = 3$, $\Delta S = 2$ is allowed in this model and the fit to the data seems to be reasonable.

It was found that the data for the transition to the 0^+ state at 7.65 MeV and the 4^+ state at 14.05 MeV could not be fitted by using this simple model. Breathing modes as discussed by Satchler[7] might be used to interpret the angular distribution for the 0^+ state. However, it should be pointed out that the ordinary distorted wave approximation method used here may also be questionable, since the magnitude of the cross section for the transition to the 2^+ state at 4.44 MeV is comparable to that for the elastic scattering beyond $\theta_{c.m.} \approx 30°$. This increases the probability of exciting higher states by two-step processes. The contributions from these processes are usually small for strong transitions but they have been found to be important for the weak states.

Use of higher terms in the interaction coupling [Eq. (2)] was also explored and the effect of this was found to be insignificant on the 2^+ state at 4.44 MeV and the 3^- state at 9.63 MeV. Their shapes did not change much; however slight changes in magnitude were found. This probably shows that the series in Eq. (2) converges rapidly.

Finally, several observations may be mentioned. It is encouraging that such a wide variety of elastic data could be well represented by a simple parametrization in the optical model. The analyses of the inelastic scattering also show that the model used is reasonably good for reproducing gross features, perhaps as good as for any other light projectile case. There is, however, much remaining ambiguity. The nature of the spin-orbit interaction is completely unknown, although it seems to be of importance. It appears that the determination of this term requires more elaborate experimental and theoretical investigation.

---

*Research supported in part by the National Science Foundation.

†Present address: Nuclear Physics Laboratory, University of Colorado, Boulder, Colorado 80302.

‡Research supported by the U. S. Atomic Energy Commission.

[1]G. T. Garvey, A. M. Smith, J. C. Hiebert, and F. E. Steigert, Phys. Rev. Lett. 8, 25 (1962).

[2]F. Videbaek, I. Chernov, R. R. Christensen, and E. E. Gross, Phys. Rev. Lett. 28, 1072 (1972).

[3]F. T. Baker and R. Tickle, Phys. Lett. 32B, 47 (1970).

[4]E. L. Petersen, I. Šlaus, J. W. Verba, R. F. Carlson, J. R. Richardson, Nucl. Phys. A102, 145 (1967).

[5]F. Hinterberger, G. Mairle, U. Schmidt-Rohr, G. J. Wagner, and P. Turek, Nucl. Phys. 115, 570 (1968).

[6]G. C. Ball and J. Cerny, Phys. Rev. 177, 1466 (1969).

[7]G. R. Satchler, Nucl. Phys. 100, 497 (1967).

[8]P. K. Bindal and K. Nagatani, to be published.

[9]K. Bethge, K. Meier-Ewert, and K. O. Pfeiffer, Z. Phys. 208, 486 (1968).

[10]A. A. Ogloblin, in *Proceedings of the International Conference on Nuclear Reactions Induced by Heavy Ions, Heidelberg, Germany, 1969*, edited by R. Bock and R. Herring (North-Holland, Amsterdam, 1970), p. 231.

[11]G. Bassani, N. Saunier, B. M. Traore, J. Raynal, A. Foti, and G. Pappalardo, Nucl. Phys. A189, 353 (1972).

[12]V. I. Chuev, V. V. Davidov, B. G. Novatskii, A. A. Ogloblin, S. B. Sakuta, and D. N. Stepanov, J. Phys. (Paris) Suppl. C6, 161 (1971).

[13]R. W. Ollerhead, C. Chasman, and D. A. Bromley, Phys. Rev. 134, B74 (1964); R. W. Ollerhead, Ph.D. dissertation, Yale University, 1963 (unpublished).

[14]Received from G. M. Lerner.

[15]F. G. Perey, Phys. Rev. 131, 745 (1963).

[16]R. H. Bassel, G. R. Satchler, R. M. Drisko, and E. Rost, Phys. Rev. 128, 2693 (1962).

[17]J. K. Dickens, F. G. Perey, and G. R. Satchler, Nucl. Phys. 73, 529 (1965).

[18]J. S. Blair, in *Proceedings of the Conference on Direct Interactions and Nuclear Reaction Mechanisms, Padua, Italy, 1962*, edited by E. Clementel and C. Villi (Gordon and Breach, New York, 1963).

[19]W. Von Oertzen, M. Liu, C. Caverzasio, J. C. Jacmart, F. Pougheon, M. Riou, J. C. Roynette, and C. Stephan, Nucl. Phys. 143, 34 (1970).

[20]P. D. Greaves, V. Hnizdo, J. Lowe, and O. Karban, Nucl. Phys. A179, 1 (1972).

[21]P. K. Bindal, J. D. Bronson, R. A. Kenefick, K. Nagatani, and D. H. Youngblood, Bull. Am. Phys. Soc. 18, 600 (1973); and to be published.

[22]W. G. Love and L. J. Parish, Nucl. Phys. A157, 625 (1970).